RSC Advances

Size dependence of the lattice parameter of carbon supported platinum nanoparticles: X-ray diffraction analysis and theoretical considerations

Journal:	*RSC Advances*
Manuscript ID:	RA-ART-05-2014-004809.R1
Article Type:	Paper
Date Submitted by the Author:	11-Jul-2014
Complete List of Authors:	Leontyev, I.; Southern Federal University, Faculty of Physics; Bayerisches Geoinstitut Universität Bayreuth, HENNET, Louis; CNRS, CEMHTI Kuriganova, Alexandra; South-Russian State Technical University, Chemical Technology Smirnova, N.; South-Russian State Technical University, Chemical Technology Dmitriev, Vladimir; ESRF, The Swiss-Norwegian Beamlines Rakhmatullin, Aydar; CNRS, CEMHTI Leontyev, Nikolay; Azov-Black See Agricultural State Academy,

Size dependence of the lattice parameter of carbon supported platinum nanoparticles: X-ray diffraction analysis and theoretical considerations

I.N. Leontyev,*[a,b,c] A.B. Kuriganova,[d] N.G. Leontyev,[e] L. Hennet,[a] A. Rakhmatullin,[a] N.V. Smirnova,[d] and V. Dmitriev[f]

Received Xth XXXXXXXXXX 20XX, Accepted Xth XXXXXXXXX 20XX
First published on the web Xth XXXXXXXXXX 200X
DOI: 10.1039/b000000x

Carbon supported Pt nanoparticles with diameters ranging from 2 to 28 nm have been studied using X-ray diffraction. Unit cell parameter of synthesized Pt/C nanoparticles is always lower s lower than that of bulk Pt. By decreasing the average particle size D to approximately 2 nm, the unit cell parameter a nonlinearly decreases by about 0.03 Åthat corresponds to a variation of 0.7% in comparison to bulk Pt and the size effect is predominant for sizes ranging from 2 to 10 nm. The dependence $a(1/D)$ is well approximated by a straight line with a slope of -0.0555±0.0067 nm^{-1} and an intercept of -3.9230±0.0017 Å. For interpreting obtained experimental dependence of unit cell parameter of Pt/C nanoparticles four different theoretical approaches such as thermal vacancy mechanism, Continuous-Medium model, Laplace pressure, and bond orderlengthstrength correlation mechanism were used. Comparison of calculated dependencies based on the above models with experimental ones shows that the Continuous-Medium model is best agreed with the unit cell parameter dependence of carbon supported Pt nanoparticles.

1 Introduction

The study of nanocrystalline materials is an active area of research in physics, chemistry and materials sciences due to their technological importance, theoretical interest and broad prospects for applications in catalysts, ferrofluids, magnetic materials, lubricants, etc. The transition from bulk crystal to nanoparticles is accompanied by a change of interatomic distances and unit cell parameters. One of the most interesting questions is the variation of the lattice parameter with decreasing particle size .

The size dependence of the lattice parameter has been studied for many years both theoretically[1–4] and experimentally. A variety of techniques, such as high resolution electron microscopy (TEM and STEM)[5–12], X-ray diffraction (XRD)[13–22], and EXAFS spectroscopy[23–29], have been used in order to investigate the nanoparticles supported on different substrates and/or coated with other materials.

The reduction of the unit cell parameter with decreasing particle size was observed for the unsupported Ag nanoparticles over the size ranges 1.3-5nm[5,6] and 3-17.8 nm[7]; and isolated nanoparticles in solid argon (size range of 2.5-13nm)[23]. However, basing on XRD studies of Ag nanoparticles (9-17nm) prepared using magnetron sputtering[13], it is found the extreme dependence of the unit cell parameter, namely, the unit cell parameter slightly increases with decreasing particle size to 12 nm, and then begins to decline. In addition, for Au (1.8÷52nm)[8], Ag (1.3÷10nm)[30], Ni (7.7nm÷bulk), Cu (0.5nm÷bulk)[27], and Pd (7nm÷bulk)[26] nanoparticles the contraction of the nearest-neighbor distance, was revealed to be a linear function of the inverse average particle size $1/D$. Reducing of the lattice parameters is also found for (i) Au nanoparticles (1.1÷6nm) prepared by vacuum evaporation[25] and (ii) Pd nanoparticles (1.4÷5nm) produced using inert gas evaporation technique[10].

Contradictory results were obtained in[14] for Ni nanoparticles in a size range of 18÷52 nm prepared by an anodic arc discharge plasma method. The lattice parameter increases significantly with decreasing grain size, and the magnitude of the lattice parameter expansion is in direct proportion to the reciprocal of the grain size. The lattice expansion resulting from the grain size reduction of Ni nanoparticles was found in the size ranges 4.9÷35 nm[15] and 7-27nm[16] as well. The bond lengths and hence lattice parameter larger than the bulk value

[a] *CNRS, CEMHTI UPR 3079, Univ. Orlans, F-45071 Orlans, France. Tel: +79185524024; E-mail: i.leontiev@rambler.ru*
[b] *LE STUDIUM, Loire Valley Institute for Advanced Studies Orleans Tours, France*
[c] *Southern Federal University, Physics Faculty, 5 Zorge str., Rostov-on-Don, 344090, Russia*
[d] *South-Russian State Technical University, 132 Prosveshenia, Novocherkassk, 346428, Russia*
[e] *Azov-Black See Agricultural State Academy, 21 Lenina str, Zernograd, Rostov Region 347740, Russia*
[f] *Swiss-Norwegian Beam Lines at ESRF, BoitePostale 220, F-38043 Grenoble, France*

have been observed for Pd nanoparticles supported on various substrates[9,11,17,28,31] and Ag nanoparticles[32].

At the same time, the study of copper clusters (1÷10 nm) embedded in solid argon[24] showed that the unit cell parameter almost corresponds to the unit cell of the bulk sample and is only slightly reduced for particles with diameters of 1.5 nm. For ligand stabilized Pd clusters, the bond lengths are close to the bulk value as well[29]. The absence of the size dependence of lattice parameter was also observed for Pb and Bi particles with $D \geq 5$nm and $D \geq 8$nm, respectively[33], as well as for Au clusters up to 6 nm[18,19,22].Thus despite the large number of studies, the existing references contains conflicting and contradictory data, and today the problem of the size dependence of the unit cell parameter is still unsolved even for face centered cubic (fcc) metals.

The same situation was observed for Pt nanoparticles. It was shown[20] that the unit cell parameter linearly decreases with decreasing particle size. In contrast, the investigations which are presented in[21,34] indicates that the unit cell parameter remains unchanged for 2.5 and 4nm nanoparticles, respectively, or even linearly increases[35] with reducing the particle size. According to Klimenkov et al *et.al.*[12], no variation in Pt-Pt distance is found for Pt nanoparticles deposited on the aluminum oxide films, when the particle size is reduced to 3 nm. However, with a further reduction of l nm, a Pt-Pt distance varies by about 10% comparing to the bulk value. On the other hand Birringer and Zimmer[36] demonstrated that the evolution of a lattice parameter as a function of the increase in the grain size for nanocrystalline Pt possesses the highly nonmonotonic behavior.

In order to contribute to the clarification of these contradictions, we have undertaken to perform XRD investigations of Pt nanoparticles ranging from 2.5 to 28 nm deposited on the carbon support. We have examined the unit cell parameter as a function of the particle size to answer the following questions: Is there a grain size dependence of the unit cell parameter and how it behaves? Our interest to study this phenomenon lies in the fact that, carbon supported platinum nanoparticles (Pt/C) are the most promising catalysts for low temperature fuel cells. It is also well known that the decrease of the interatomic distance Pt-Pt (i.e. unit cell parameter) is one of the reason of the positive influence on the catalytic activity toward the oxygen reduction reaction, since that facilitates dissociative hemosorption of oxygen atoms[37–39].

2 Experimental

We applied three different techniques which allowed us to synthesize Pt nanoparticles in a wide range of sizes (from 2.5 to 28 nm). For all of them, we used both Vulkan XC-72 (Cabot Corp., 240 $m^2 \cdot g^{-1}$) and Timrex HSAG-300 (TIMCAL, 250 $m^2 \cdot g - 1$) as carbon supports.

The two first methods are based on the reduction of the metal precursor (hexachloroplatinic acid $H_2PtCl_6 \cdot 6H_2O$) by different reducing agents. To prepare the catalysts ethylene glycol aqueous solution was mixed with the 2 % H_2PtCl_6 solution at different temperatures between 80 and 130∘C and a colloidal solution was synthesized during 3 h. Then the carbon support were added into the reaction system and the synthesis was continued for 2 h. Pt nanoparticles were also prepared by the reduction of oxalic acid. Before Pt-precursor deposition carbon support was pre-treated with 4 M oxalic acid aqueous solution under stirring at 80°C during 15 min. Such acid treatment creates different functional groups (hydroxyl and/or carboxyl) at the carbon support surface, which facilitate a discharge of the metal complexes on surface of carbon support. After the acid activation of the carbon support 2 % H_2PtCl_6 metal salt solution was injected into the carbon suspension and the synthesis was performed during 5 h at a constant temperature. Finally the third method we use is the dispergation of Pt foil by pulse alternating current in water solutions with different concentration K and NaOH. A detailed description of this method can be found in our previous work[40]. After the synthesis supported Pt/C catalyst was separated from the solution by filtering, then it was washed with water, and finally dried overnight at 70°C.

Synchrotron XRD measurements were carried out in the Debye-Scherrer geometry at the Swiss-Norwegian Beam Lines (SNBL) at ESRF (Grenoble, France) with a radiation of wavelength λ=0.77Åand a MAR345 image-plate detector. The wavelength, sample-to-detector distance (95 mm) and resolution of the setup were calibrated with standard specimen of LaB6 (Standard Reference Materials 660a, National Institute for Standards and Technology, Gaithersburg, USA NIST) powder. Samples were placed into glass capillaries (Hilgenberg GmbH) (diameter 0.3 mm) with a 0.01 mm wall thickness. Data were processed with the Fit2D software[41]. The peak shapes were described by the pseudo-Voigt function[42]. The X-ray reflections were fitted using the Winplotr module of the FullProf software[43]. Fitting of the reflections from the synthesized samples was implemented taking into account the reflections of the carbon support[44]. The corrections for the instrumental broadening were made according to a conventional procedure described in[45]. The average particle size D_v was determined using the Sherrer equation[46]: $D_v = K\lambda/(H_{Pv}\cos\theta)$, where λ is the wavelength, θ - Bragg angle, and K = 0.89 Sherrer constant. The fitting results (111) peak were employed to estimate the average particle size, and the unit cell parameter was calculated using the UNITCELL software[47].

3 Results and Discussion

The series of the carbon-supported Pt samples with different average sizes were investigated to determine the size depen-

dence of the unit cell parameter $a(D)$. Selected XRD patterns corresponding to average particle sizes of 3.1, 5.7 and 11.5 nm are presented in Fig. 1. As for all investigated samples, they show only broadened peaks corresponding to planes (111), (200), (220), (311) and (222), characteristic of the fcc structure of Pt.

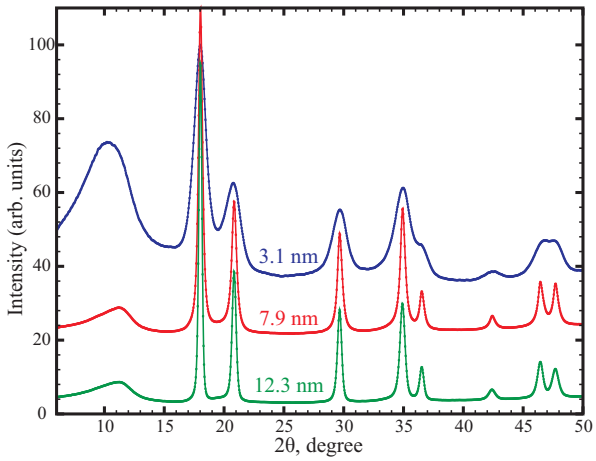

Fig. 1 Selected XRD powder patterns of carbon supported Pt nanoparticles for 3 particle sizes (3.1, 5.7 and 11.5nm).

Figure 2 presents the evolution of the lattice parameter a of all as-prepared samples as a function of the particle size (circle symbols). Obviously, it is always lower than the value of the bulk Pt value (3.9231Å). By decreasing the average particle size D to about 2 nm, the unit cell parameter a decreases by about 0.03 Åthat corresponds to a variation of 0.7% in comparison to bulk Pt. It can be seen that the size effect is predominant for the sizes ranging from 2 to 10 nm. When the size is bigger than 20 nm, the changes are relatively small and can be neglected. Furthermore, it should be noted that the dependence $a(1/D)$ is well approximated by a straight line with a slope of -0.0555±0.0067 nm^{-1} and an intercept of -3.9230±0.0017 Å(correlation coefficients was 0.9). This intercept value is consistent with the unit cell parameter of bulk Pt.

As reported in many papers on the synthesis and study of the properties of platinum based alloy catalysts, the shift of the Pt diffraction peaks to higher 2θ values is only attributed to the formation of a Pt alloy[48–50].

Obtained $a(D)$ dependence indicates that in Pt-based catalysts the reduction of unit cell parameter can be caused not only by the influence of the alloying component, but also by decreasing the average particle size. Besides, the unit cell parameter of a bulk sample is used to calculate, by Vegard's law, the concentration of the alloying component in carbon supported Pt-Metal catalysts[51]. However, we believe, that neglecting the size dependence of the unit cell parameter can

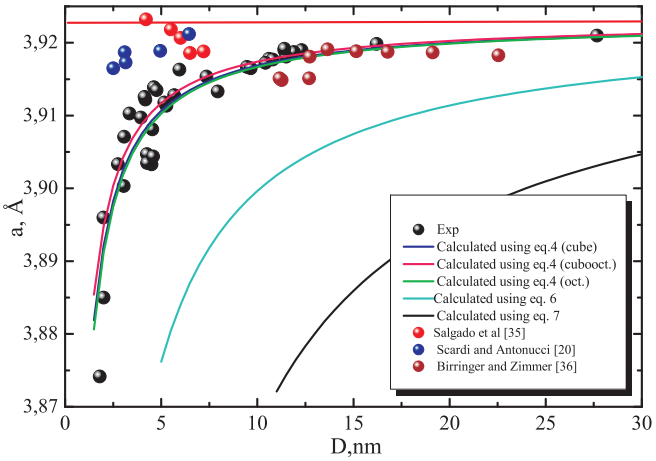

Fig. 2 The experimental (1) and calculated (lines 2-6) unit cell parameters of carbon supported Pt nanoparticles as a function of the average particle size D. Experimental dependence also contains data obtained in Ref.[54] $a(D)$ dependencies obtained by Salgado et al [35], Scardi and Antonucci [20], and Birringer and Zimmer [36] are shown as well

lead to erroneous results. Indeed, with Pt bulk samples doped by nickel, the reduction of the particle size to ∼2 nm leads to a decrease of the unit cell parameter by ∼20%[52]. It should also be noted that we observed a similar nonlinear particle size dependence of the unit cell parameter in Co-doped carbon supported Pt nanoparticles the same composition[53].

Based on various assumptions, several models describing the particle size dependence of the unit cell parameter have been established. One of them assume that the reduction of the lattice parameters is due to the formation of a large number of vacancies by decreasing the particle size[55–57]. The formation of these vacancies in a nanoparticle system compared to the bulk metal leads to the reduction of the lattice parameter of a cluster that is related to the vacancy concentration:

$$\Delta a = \frac{1}{3} a_{bulk} c_v \left(1 - \frac{V_v}{\Omega}\right) \quad (1)$$

where c_v is the vacancy concentration, Δa is the change of the lattice parameter due to vacancies, Ω is the atomic volume of a defect free crystal, and V_v is the change of the atomic volume caused by the presence of one vacancy. It is known that the equilibrium vacancy concentration is as follows[58]:

$$c_v(D,T) = c_0 exp\left(\frac{E_v(D)}{k_B T}\right) \quad (2)$$

where $c_0 = exp(S_F/k_B)$ is the size-independent preexponential coefficient, S_F the formation entropy, k_B is the Boltzmann constant, T is the absolute temperature and $E_v(D)$ is the size

dependent vacancy formation energy described by the following equation[59]:

$$E_v(D) = E_v \frac{2D/h-2}{2D/h-1} exp\left(-\frac{2S_b}{3R(2D/h-1)}\right), \quad (3)$$

where, E_v is the vacancy formation energy for the bulk material, $S_b = E_b/T_b$ is the bulk evaporation entropy of crystals with E_b and $T_b(\infty)$ being respectively, the bulk cohesive energy and the evaporation temperature, h is the atomic diameter and R is the ideal gas constant. Using the parameters summarized in Tables 1 and Equations (1) to (3) we estimated the vacancy concentration and the corresponding dilatation of the unit cell parameter for Pt nanoparticles down to 2 nm. This calculation shows that for Pt nanoparticles with an average particle size of 2 nm, the vacancy concentration is $1.15 \cdot 10^{-9}$ at ambient condition. It is in 10^{12} times higher than for the bulk sample. But the corresponding variation of the unit cell parameter is only $2.7 \cdot 10^{-9}$ Åthat is significantly lower than experimentally observed even for carbon supported Pt nanoparticles with a 27 nm size.

Table 1 The relevant data used in the calculations.

h /nm	V_v/Ω,	S_F/k_B	E_b /$KJ \cdot mol^{-1}$	T_b/K
2.78	0.76[58]	4.5[58]	564[60]	4098[60]

A second model which describes the size and shape dependence of lattice parameters of metallic nanoparticles is the so-called Continuous-Medium (CM) model developed by Qi and Wang[1]. They have assumed that a nanoparticle is formed in three steps: (i) a particle is taken out from an ideal bulk crystal without changing the structure, (ii) the surface tension of the particle contracts elastically, and (iii) a nanoparticle is formed in equilibrium condition. Thus, by minimizing the sum of the increased surface energy and the elastic energy, an expression for calculating the lattice parameters of metallic nanoparticles is obtained as follows

$$a(D) = a_{bulk}\left(1 - \frac{1}{1+\sqrt{\alpha}GD/\gamma}\right) \quad (4)$$

where $a(D)$ is the unit cell parameter of the particle having size D, G is the shear modulus, γ is the surface energy and $\alpha = S_{pol}/S_{sph}$ is the shape factor which is defined as the ratio of the surface area of a nonspherical nanoparticle S_{pol} to that of a spherical nanoparticle S_{sph}, where both nanoparticles have identical volume. The calculation of the size dependence was performed only for 3 types of polyhedron: cube, cubooctahedron and octahedron, since, as demonstrated in our previous work[54] and also illustrated in numerous review articles[61–63], the shape of the carbon supported Pt nanoparticles synthesized without using any capping agent is the Wullfs polyhedra that corresponds to perfect polyhedra (cubes, octahedra) and their truncated modifications. The shape factors $\alpha = S_{pol}/S_{sph}$ for three mentioned configurations are listed in Table 2. To estimate the size and shape dependencies of the lattice parameter according to Eq.(4), we used the parameters listed in Table 2 and 3. The evolutions of $a(D)$ calculated using Eq.(4) are depicted in Fig.2. All three calculated dependences coincide with the experimental ones. In other words, for Wullfs polyhedron, the particles shape is not appreciably affected by the variation of the unit cell parameter with decreasing the nanoparticles size down to 2 nm.

Table 2 Full surface area S, volume V and shape factor α for the different Wullfs polyhedra

Polyhedron	S	V	α
Cube	$6a^2$	a^3	$\frac{3}{2\pi}(\frac{4\pi}{3})^{2/3} = 1.241$
Cubooctahedron	$(3+\sqrt{3})a^2$	$\frac{5}{6}a^3$	$\frac{3+\sqrt{3}}{4\pi}(\frac{8\pi}{5})^{2/3} = 1.105$
Octahedron	$\sqrt{3}a^2$	$\frac{a^3}{6}$	$\frac{\sqrt{3}}{4\pi}(8\pi)^{2/3} = 1.183$

Another approach which is usually used for explaining the size dependence of the unit cell parameters is based on the notion that the nanoparticles are compressed by the Laplace pressure. The value for the pressure difference of a spherical surface was formulated in 1805 independently by Thomas Young and Pierre Simon de Laplace, giving the LaplaceYoung equation:

$$\triangle P = 2fS/(3V) = 4f/D,$$

where D is the average particle size, f is the interface stress, S is the particle surface area, and $\triangle P$ is the difference of pressure inside and outside the particle. From a mechanical point of view, the hydrostatic pressure on the surface of nanoparticles induced by the intrinsic surface stress results in lattice contraction or a lattice strain $\varepsilon(D) = (a_{bulk} - a(D))/a_{bulk}$. Using the definition of the compressibility $k = -\triangle V/(VP)$, $\varepsilon = \triangle D/D = \triangle S/(2S) = \triangle V/(3V)$ under small strain ($\triangle$ denotes the difference) and $S/V = 6/D$, we obtain:

$$\varepsilon = -4kf/(3D), \quad (5)$$

According to the LaplaceYoung equation and considering a size-dependence of the solid-liquid interface energy, the relative change of the lattice constants $a(D)$ at room temperature for the nanoparticles can be expressed as[3]

$$a(D) = a_{bulk}\left(1 - \frac{14}{(3T_m/T+6)D}\sqrt{\frac{kD_0hS_{vib}H_m}{RV_m}}\right) \quad (6)$$

where T_m and H_m are the melting temperature and the enthalpy of bulk crystals, respectively, S_{vib} is the vibrational part of the overall melting entropy S_m, V_m is the molar volume and T is the absolute temperature.

Table 3 The relevant data used in the calculations.

G/Pa	γ_{111} /$J\cdot m^{-2}$	γ_{100} /$J\cdot m^{-2}$	k·10^{-12}/Pa^{-1}	T_m/K	V_m /$cm^3\cdot mol^{-1}$	H_m /$kJ\cdot mol^{-1}$
168[60]	2.299[64]	2.734[64]	3.62[60]	2045[60]	9.1[60]	22[60]

The particle size dependence of the unit cell parameter determined from Eq.(6) is shown in Fig.2 (cyan line). For this calculation, we used the thermodynamic and physical properties listed in Table 3. The analysis of Fig.2 shows that the experimental dependence of the unit cell parameter of carbon supported Pt nanoparticles is not well described by the dependence calculated by Eq.(6) in comparison with that determined using Eq.(4). Actually, this approach which is based on the action of the Laplace pressure can be confronted to various difficulties, despite it correctly described the reduction of the lattice parameter observed experimentally for Ag[5,6,23], Pd[10,26] and Au nanoparticles[25,65]. For example, if the Laplace pressure compresses nanoparticles, hence the observed external pressure for a phase transition in nanoparticles should be smaller than for bulk samples and the general rule seems to be as follows: the smaller the nanoparticles, the higher the transformation pressure. However, the size evolution for pressure-induced γ-Fe_2O_3(maghemite) to Fe_2O_3 (hematite) transition showed that 7-nm nanocrystals at 27 GPa, transforms to 5-nm ones at 34 GPa, and to 3-nm ones at 37 GPa[66], i.e. the tendency is opposite. For Ge nanoparticles[67] the transition pressure increases with decreasing particle size as well as for Al_2O_3[68], AlN[69], and ZnO[70].

A critical analysis of the Laplace pressure was performed in details in[71–74]. The Laplace pressure was shown to be a formal quantity that makes it possible to express the chemical potential of the particle $\mu(D,P)$ through the chemical potential of the corresponding infinite (massive) sample $\mu(\infty,P+P_L)$ compressed by a pressure equal to the Laplace pressure P_L for a particle. Thus, it was concluded that the Laplace pressure is a purely mathematical concept and cannot cause compression of bodies. Moreover, based on theoretical calculations, it is suggested in[75,76] that the reason of changes in interatomic distances observed in nanoparticles can be explained by the phenomenon of surface multilayer relaxation that observed on the surface of macroscopic metallic crystals. Although, the relaxation usually embraces only a few surface layers, it causes an amendment to the thermodynamic quantities of the nanoparticles of $\sim 1/D$, and they are similar in size dependence with amendments arising from the introduction of the Laplace pressure.

Based on this surface relaxation phenomenon Sun proposed the bond orderlengthstrength (BOLS) correlation mechanism for determining the size dependence of the nanoparticles parameters such as melting temperature, Debye temperature, Youngs modulus etc.[77,78]. The key idea of the BOLS mechanism is that the nanomaterials possess a large proportion of surface atoms with bond-order deficiency compared to the bulk counterpart. As a result, surface skin composed of three atomic layers often relaxes and reconstructs without exception, that critically affects the physical and chemical properties in the skin. In terms of this mechanism[77], the lattice strain in specific atom layer is given by the following expression:

$$\varepsilon_i = d_i/d = C_i - 1$$

where $C_i = 2/1+exp[(12-z_i)/(8z_i)]$ is the coefficient of bond contraction, subscript i denote an atom in the i^{th} atomic layer. The index i is counted up to three from the outermost atomic layer[79]. The parameter z_i is the effective coordination numbers of the specific i-th atom, and it varies with the size and the curvature of the nanostructure in an empirical way $z_1 = 4(1-0.75/K_j)$, $z_2 = z_1+2$, and $z_3 = 12$ with $K_j = R_j/d$ being the dimensionless form of nanosolid size, which corresponds to the number of atoms K_j, with mean diameter or bond length d, lined up along the radius R_j of a spherical-like nanosolid. Finally the size-dependent average lattice constant of the nanoparticles can be expressed by the BOLS model

$$a(D) = a_{bulk}\left(1-\sum_{i=1}^{3}\frac{3}{K_j}C_i(C_i-1)\right) \quad (7)$$

The corresponding $a(D)$ dependence calculated using Eq.(7) is depicted in Fig.2(black line). The essential difference between the experiment and the simulation may be attributed to the following reasons. First of all, oxygen chemisorption could expand the first metallic interlayer by up to 10÷25% though the oxygenmetal bond contracts[80]. Second, considerable experimental and theoretical calculations data[81–83] indicate that multilayer relaxation of surfaces does not fall monotonically but undergoes oscillations. In other words, the surface relaxation can be of variable sign. Both of these reasons can induce a smaller reduction of the unit cell parameter with the decrease of the nanoparticles size.

4 Conclusions

Carbon supported Pt nanoparticles with diameters ranging from 2 to 28 nm have been studied using X-ray diffraction. The unit cell parameter of the synthesized Pt/C nanoparticles is always lower than the value of bulk Pt (3.9231Å). By decreasing the average particle size D down to approximately 2 nm, the unit cell parameter a decreases nonlinearly

by about 0.03 that corresponds to the variation of 0.7% in comparison to bulk Pt and the size effect is predominant for sizes ranging from 2 to 10 nm. The dependence of the lattice parameter as a function of inverse average particle size $a(1/D)$ is well approximated by a straight line with a slope of -0.0555±0.0067 nm^{-1} and an intercept of -3.9230±0.0017 Å. For interpreting the obtained experimental dependence of the unit cell parameter of Pt/C nanoparticles, 4 different theoretical approaches were used, including thermal vacancy mechanism, Continuous-Medium model, Laplace pressure, and bond orderlengthstrength correlation mechanism. The comparison of the calculated dependencies based on the above models with the experimental data, shows that the results provided by the the Continuous-Medium model is in better agreement than those obtained by others approaches. It is thus the best approach to simulate the unit cell parameter dependence of carbon supported Pt nanoparticles.

5 Acknowledgements

We thank SNBL ESRF for the access to the synchrotron radiation facility. This work was financially supported by Russian Foundation for Basic Research (project 12-08-01193-a)and Ministry of Education and Science of Russian Federation (project 2945 of State Order 2014/143).

References

1 W. H. Qi and M. P. Wang, *J. Nanopart. Res.*, 2005, **7**, 51–57.
2 W. H. Qi, B. Y. Huang, M. P. Wang, Z. M. Yin and J. Li, *J. Nanopart. Res.*, 2009, **11**, 575–580.
3 Q. Jiang, L. H. Liang and D. S. Zhao, *J. Phys. Chem. B*, 2001, **105**, 6275–6277.
4 Y. H. Medasani, B.and Park and I. Vasiliev, *Phys. Rev. B*, 2007, **75**, 235436–.
5 M. Dubiel, H. Hofmeister and E. Schurig, *Phys. Status Solidi B*, 1997, **203**, R5–R6.
6 H. Hofmeister, S. Thiel, M. Dubiel and E. Schurig, *Appl. Phys. Lett.*, 1997, **70**, 1694–1696.
7 H. Wasserman and J. Vermaak, *Surf. Sci.*, 1970, **22**, 164–172.
8 J. S. Vermaak and D. Kuhlmann-Wilsdorf, *J. Phys. Chem.*, 1968, **72**, 4150–4154.
9 K. Heinemann and H. Poppa, *Surf. Sci.*, 1985, **156, Part 1**, 265–274.
10 R. Lamber, S. Wetjen and N. I. Jaeger, *Phys. Rev. B*, 1995, **51**, 10968–10971.
11 R. Lamber, N. Jaeger and G. Schulz-Ekloff, *Surf. Sci.*, 1990, **227**, 15–23.
12 M. Klimenkov, S. Nepijko, H. Kuhlenbeck, M. Bumer, R. Schlgl and H. J. Freund, *Surf. Sci.*, 1997, **391**, 27 – 36.
13 I. Shyjumon, M. Gopinadhan, O. Ivanova, M. Quaas, H. Wulff, C. A. Helm and R. Hippler, *Eur. Phys. J. D*, 2006, **37**, 409–415.
14 Z. Wei, T. Xia, J. Ma, W. Feng, J. Dai, Q. Wang and P. Yan, *Mater. Charact.*, 2007, **58**, 1019 – 1024.
15 M. Y. Gamarnik, *Phys. Status Solidi B*, 1991, **168**, 389–395.
16 Y. Duan and J. Li, *Mater. Chem. Phys.*, 2004, **87**, 452–454.
17 K. Ohshima, S. Yatsuya and J. Harada, *J. Phys. Soc. Jpn.*, 1981, **50**, 3071–3074.
18 J. Harada and K. Ohshima, *Surf. Sci.*, 1981, **106**, 51 – 57.
19 J. Harada, S. Yao and A. Ichimiya, *J. Phys. Soc. Jpn.*, 1980, **48**, 1625–1630.
20 P. Scardi and P. Antonucci, *J. Mater. Res.*, 1993, **8**, 1829–1835.
21 E. Moroz, S. Bogdanov and V. Ushakov, *React. Kinet. Catal. Lett.*, 1978, **9**, 109–112–.
22 K. Ohshima and J. Harada, *J. Phys. C: Solid State Phys.*, 1984, **17**, 1607.
23 P. A. Montano, W. Schulze, B. Tesche, G. K. Shenoy and T. I. Morrison, *Phys. Rev. B*, 1984, **30**, 672–677.
24 P. A. Montano, G. K. Shenoy, E. E. Alp, W. Schulze and J. Urban, *Phys. Rev. Lett.*, 1986, **56**, 2076–2079.
25 A. Balerna, E. Bernieri, P. Picozzi, A. Reale, S. Santucci, E. Burattini and S. Mobilio, *Phys. Rev. B*, 1985, **31**, 5058–5065.
26 C.-M. Lin, T.-L. Hung, Y.-H. Huang, K.-T. Wu, M.-T. Tang, C.-H. Lee, C. T. Chen and Y. Y. Chen, *Phys. Rev. B*, 2007, **75**, 125426–.
27 G. Apai, J. F. Hamilton, J. Stohr and A. Thompson, *Phys. Rev. Lett.*, 1979, **43**, 165–169.
28 C. Goyhenex, C. R. Henry and J. Urban, *Philos. Mag. A*, 1994, **69**, 1073–1084.
29 R. Benfield, A. Filipponi, D. Bowron, R. Newport, S. Gurman and G. Schmid, *Physica B*, 1995, **208-209**, 671–673.
30 W. Cai, H. Hofmeister and M. Dubiel, *Eur. Phys. J. D*, 2001, **13**, 245–253.
31 C. Kuhrt and R. Anton, *Thin Solid Films*, 1991, **198**, 301–315.
32 S. Onodera, *J. Phys. Soc. Jpn.*, 1992, **61**, 2190–2193.
33 A. Yokozeki and G. D. Stein, *J. Appl. Phys.*, 1978, **49**, 2224–2232.
34 P. Yu, M. Pemberton and P. Plasse, *J. Power Sources*, 2005, **144**, 11–20.
35 J. R. C. Salgado, J. J. Quintana, L. Calvillo, M. J. Lazaro, P. L. Cabot, I. Esparbe and E. Pastor, *Phys. Chem. Chem. Phys.*, 2008, **10**, 6796–6806.
36 R. Birringer and P. Zimmer, *Acta Mater.*, 2009, **57**, 1703 – 1716.
37 M.-k. Min, J. Cho, K. Cho and H. Kim, *Electrochim. Acta*, 2000, **45**, 4211–4217.
38 E. Antolini, J. Salgado, M. Giz and E. Gonzalez, *Int. J. Hydrogen Energy*, 2005, **30**, 1213–1220.
39 X. Wang, Y. Orikasa, Y. Takesue, H. Inoue, M. Nakamura, T. Minato, N. Hoshi and Y. Uchimoto, *J. Am. Chem. Soc.*, 2013, **135**, 5938–5941.
40 I. Leontyev, A. Kuriganova, Y. Kudryavtsev, B. Dkhil and N. Smirnova, *Appl. Catal., A*, 2012, **431–432**, 120–125.
41 A. P. Hammersley, S. O. Svensson, M. Hanfland, A. N. Fitch and D. Hausermann, *High Pressure Res.*, 1996, **14**, 235–248.
42 P. Thompson, D. E. Cox and J. B. Hastings, *J. Appl. Crystallogr.*, 1987, **20**, 79–83.
43 T. Roisnel and J. Rodriguez-Carvajal, Materials Science Forum, Proceedings of the Seventh European Powder Diffraction Conference (EPDIC 7), 2000, pp. 118–123.
44 I. Leontyev, D. Y. Chernyshov, V. Guterman, E. Pakhomova and A. Guterman, *Appl. Catal., A*, 2009, **357**, 1–4.
45 S. Vives, E. Gaffet and C. Meunier, *J. Mater. Sci. Eng. A*, 2004, **366**, 229–238.
46 L. E. Klug, H. P.; Alexander, *X-ray Diffraction Procedures from Polycrystalline and Amorphous Materials*, John Wiley: New York, 1974.
47 T. J. B. Holland and S. A. T. Redfern, *J. Appl. Crystallogr.*, 1997, **30**, 84.
48 J. Zeng and J. Y. Lee, *J. Power Sources*, 2005, **140**, 268–273.
49 J. Salgado, E. Antolini and E. Gonzalez, *J. Power Sources*, 2004, **138**, 56–60.
50 H. Yang, C. Coutanceau, J.-M. Leger, N. Alonso-Vante and C. Lamy, *J. Electroanal. Chem.*, 2005, **576**, 305–313.
51 Z. Xu, H. Zhang, S. Liu, B. Zhang, H. Zhong and D. S. Su, *Int. J. Hydrogen Energy*, 2012, **37**, 17978–17983.
52 L. I. Mirkin, *X-ray control of engineering materials*, Moscow, 1979.
53 I. Leontyev, V. Guterman, E. Pakhomova, P. Timoshenko, A.V.Guterman, I. Zakharchenko, G. Petin and B. Dkhil, *J. Alloys Compd.*, 2010, **500**, 241–246.

54 I. N. Leontyev, S. V. Belenov, V. E. Guterman, P. Haghi-Ashtiani, A. P. Shaganov and B. Dkhil, *J. Phys. Chem. C*, 2011, **115**, 5429–5434.

55 V. D. Borman, P. V. Borisyuk, I. V. Tronin, V. N. Tronin, V. I. Troyan, M. A. Pushkin and O. S. Vasiliev, *Int. J. Mod. Phys. B*, 2009, **23**, 3903–3911.

56 X. F. Yu, X. Liu, K. Zhang and Z. Q. Hu, *J. Phys.: Condens. Matter*, 1999, **11**, 937.

57 W. Hertz, W. Waidelich and H. Peisl, *Phys. Lett. A*, 1973, **43**, 289 – 290.

58 Y. Kraftmakher, *Phys. Rep.*, 1998, **299**, 79–188.

59 C. C. Yang and S. Li, *Phys. Rev. B*, 2007, **75**, 165413.

60 http://environmentalchemistry.com/yogi/periodic/Pt.html.

61 Z. Peng and H. Yang, *Nano Today*, 2009, **4**, 143–164.

62 L. Carbone and P. D. Cozzoli, *Nano Today*, 2010, **5**, 449–493.

63 J. Chen, B. Lim, E. P. Lee and Y. Xia, *Nano Today*, 2009, **4**, 81–95.

64 L. Vitos, A. Ruban, H. Skriver and J. Kollar, *Surf. Sci.*, 1998, **411**, 186–202.

65 T. Comaschi, A. Balerna and S. Mobilio, *J. Phys.: Conf. Ser.*, 2009, **190**, 012122–.

66 S. M. Clark, S. G. Prilliman, C. K. Erdonmez and A. P. Alivisatos, *Nanotechnology*, 2005, **16**, 2813–.

67 H. Wang, J. F. Liu, Y. He, Y. Wang, W. Chen, J. Z. Jiang, J. S. Olsen and L. Gerward, *J. Phys.: Condens. Matter*, 2007, **19**, 156217–.

68 B. Chen, D. Penwell, L. R. Benedetti, R. Jeanloz and M. B. Kruger, *Phys. Rev. B*, 2002, **66**, 144101–.

69 A. Srivastava and N. Tyagi, *J. Phys.: Conf. Ser.*, 2012, **377**, 012066–.

70 S. Li, Z. Wen and Q. Jiang, *Scr. Mater.*, 2008, **59**, 526–529.

71 E. L. Nagaev, *phys. stat. sol. (b)*, 1991, **167**, 381–404.

72 E. Nagaev, *Phys. Rep.*, 1992, **222**, 199–307.

73 V. I. Gorchakov, E. L. Nagaev and S. P. Chizhik, *Fiz. Tverd. Tela*, 1988, **30**, 1068–1075.

74 E. Nagaev, *Phys.-Usp.*, 1992, **162(9)**, 49–124.

75 P. Jiang, F. Jona and P. M. Marcus, *Phys. Rev. B*, 1987, **36**, 6336–6338.

76 V. I. Gorchakov, L. K. Grigorieva, E. L. Nagaev and S. P. Chizhik, *Zhurnal Eksperimentalnoi I Teoreticheskoi Fiziki*, 1987, **93**, 2090–2101.

77 C. Q. Sun, *Prog. Solid State Chem.*, 2007, **35**, 1–159.

78 C. Q. Sun, B. K. Tay, X. T. Zeng, S. Li, T. P. Chen, J. Zhou, H. L. Bai and E. Y. Jiang, *J. Phys.: Condens. Matter*, 2002, **14**, 7781–.

79 W. J. Huang, R. Sun, J. Tao, L. D. Menard, R. G. Nuzzo and J. M. Zuo, *Nat. Mater.*, 2008, **7**, 308–313.

80 J. Van Der Veen, R. Smeenk, R. Tromp and F. Saris, *Surf. Sci.*, 1979, **79**, 212–218.

81 J. Wan, Y. L. Fan, D. W. Gong, S. G. Shen and X. Q. Fan, *Modell. Simul. Mater. Sci. Eng.*, 1999, **7**, 189–.

82 V. Zolyomi, J. Koller and L. Vitos, *Philos. Mag.*, 2008, **88**, 2709–2714.

83 N. E. Singh-Miller and N. Marzari, *Phys. Rev. B*, 2009, **80**, 235407–.